Formulation and characterization of bixin-loaded microparticles using ionic gelation method

Bienvenido Balotro¹, Sean Paul Rojo¹, Keane Mc Josef Ku¹, Jude Benedick Acedera¹, Ma. Cailah Joyce Velasco¹, Cherika Eunyce Catalogo¹, Danielle Justinne Clemente¹, Shanna Nicole Ong¹, Bryan Paul Bulatao^{1,2}, Patrick Junard Regidor¹, Czarina Dominique Delos Santos¹, Ethel Andrea Ladignon¹, Jocelyn Palacpac¹, Julius Andrew Nuñez³, and Clinton Gomez*¹

¹Department of Industrial Pharmacy, College of Pharmacy, University of the Philippines Manila ²Institute of Pharmaceutical Sciences, National Institutes of Health, University of the Philippines Manila ³Laboratory of Materials, Department of Physical Sciences and Mathematics, College of Arts and Sciences, University of the Philippines Manila

ABSTRACT

ormulations of bixin-loaded chitosan-tripolyphosphate hyaluronic acid-coated microparticles (BX-CS/TPP-HA MP) were prepared using the ionic gelation method. Encapsulating BX in MPs aims to address BX's poor solubility and dispersion in aqueous media. The effects of BX concentration, CS:TPP ratio, and HA concentration on the formulation of BX-CS/TPP-HA MPs were investigated using a one-factor-at-a-time approach, with particle size, polydispersity index (PDI), zeta potential, encapsulation efficiency (EE), and loading capacity (LC) as the quality attributes. To further characterize the MPs, scanning electron microscopy (SEM) and Fourier transform infrared (FTIR) spectroscopy were conducted. A formulation of BX-CS/TPP-HA MP containing 9 mg/mL BX, 4:1 CS:TPP, and 0.3% w/v HA resulted in less than 1000 µm particle

size, acceptable PDI, and zeta potential within the range -20 to -40 mV, as determined with a dynamic light scattering analyzer. The results of the EE and LC confirm the successful BX loading. SEM analysis revealed spheres with sizes ranging from 150 to 400 μ m, indicating the microparticulate nature of the BX-CS/TPP-HA. The FTIR spectroscopy results further confirm that BX was successfully loaded into the BX-CS/TPP-HA MPs. The results of this formulation study can be utilized for addressing formulation issues related to BX's solubility and stability in a dispersed system.

INTRODUCTION

Bixin (BX) is a natural pigment found in the outer layer seeds of *Bixa orellana*. It belongs to the carotenoid family, which gives a high range of colors that include yellow, orange, and red hues (Husa et al., 2018). Its carotenoid content has served a significant role in the medicinal and industrial use of annatto seeds (de Oliveira Júnior et al., 2019). In addition, it also has the approval of the US FDA to be used as an edible colorant in food products

Email Address: cbgomez@up.edu.ph

Date received: 30 April 2025

Dates revised: 17 June 2025 and 18 August 2025

Date accepted: 20 September 2025

DOI: https://doi.org/10.54645/2025182CGN-77

KEYWORDS

Bixin, Microparticle, Formulation, One-factor-at-a-time, Ionic gelation

^{*}Corresponding author

(Moreira et al., 2014). BX exhibits antioxidant, anti-inflammatory, lung-protective, and hepatoprotective properties (Tao et al., 2015). One of the potential applications of BX is for the treatment and prevention of retinal diseases (Camelo et al., 2020; Tsuruma et al., 2012). Formulating BX as a microparticle (MP) is accomplished by a microencapsulating technique that involves forming an encapsulating matrix between 1 and 1000 µm in diameter. It provides good quality and stable microparticles at a resource-efficient cost.

MP formulations, like nanoparticles, can also help minimize toxicity and adverse effects by accumulating drugs at target sites, thereby reducing the required dosage of the active compound (Yusuf et al., 2023). According to the EFSA Panel on Food Additives and Nutrient Sources (2016), there is a derived acceptable daily intake (ADI) of 6 mg of BX per kg of body weight and exposure estimations were placed way below the ADI across all population groups, proving its safety. Attempts were made to deliver drugs into the posterior segment of the eye using MP eye drop formulations developed on γ-cyclodextrin (γCD)-based nanoparticle agglomerates (Stefansson, 2022) or topical dexamethasone-cyclodextrin MP (Tanito et al., 2011), chondroitin sulfate (Bonferoni et al., 2007), and chitosan (Dragostin et al., 2022). Drug delivery into the posterior eye segment requires negatively charged MP barriers due to the negatively charged nature of the vitreous humor (del Amo et al., 2017). Anionic MP can experience repulsion from negative charges present on corneal and conjunctival surfaces, resulting in easier diffusion into the retina. On the contrary, cationic particles have a greater tendency for phagocytosis into the mononuclear phagocytic system (del Amo et al., 2017), necessitating the addition of a second anionic coating material like hyaluronic acid (HA) to prevent further inflammation (Dovedytis et al., 2020). Concentrations of HA, chitosan (CS), and tripolyphosphate (TPP) must be controlled, based on previous studies, to avoid overloading associated with MP bursting. HA concentration (Espinosa-Cano et al., 2021) and CS concentration (Des Bouillons-Gamboa et al., 2024) impact the MP size. TPP ensures MP structure stabilization due to interactions with the amino groups of CS (Kim et al., 2022).

However, poor dispersion system stability marked by agglomeration and macroparticle formation is the main challenge in an enclosed matrix with BX.

Overcoming this problem involves the formulation of BX-loaded CS-TPP HA-coated microparticles (BX-CS/TPP-HA MP) using the ionic gelation method (Kim et al., 2022), exploring formulation and process parameters that can be further investigated. The ionic gelation method was utilized due to its simplicity and efficiency compared to other encapsulation techniques. The method can

proceed without sophisticated equipment and expensive reagents, with reduced processing times.

MATERIAL AND METHODS

Materials

BX powder 40% (CAS No. 6983-79-5) was purchased from Amitychem Corporation. CS (CAS No. 9012-76-4) was purchased from Hangzhou Dingyan Chem Co. Ltd. HA (CAS 9004-61-9) was acquired from HeBei GuanLang (Crovell) Biotechnology Co., Ltd.; and lastly, absolute ethanol, glacial acetic acid, sodium TPP, and Tween 80 were all acquired from DKL Laboratory Supplies.

Preparation of the BX-CS/TPP Dispersion

The BX solution was prepared by dissolving powdered BX in absolute ethanol to achieve a concentration range of 6 to 13.5 mg/mL (Table 1). The CS solution was prepared by dissolving various amounts of CS (Table 1) in 100 mL of 1% acetic acid. Subsequently, an aliquot of 30 mL was taken, followed by the addition of 0.6 mL Tween 80. The TPP solution was prepared by dissolving 0.1 g TPP in 100 mL of distilled water. The pH of the CS solution and the TPP solution was adjusted to pH 5 by adding appropriate volumes of 8N sodium hydroxide or 2N acetic acid. The HA solution was prepared by dissolving varying quantities of HA (Table 1) in an acetate buffer (pH 5).

To prepare the BX-CS dispersion, the BX solution was loaded into a syringe, and 1 mL was added dropwise at a flow rate of 1 mL/min using a G21, 1-inch syringe needle into a 30 mL CS solution under continuous stirring at 1800 rpm with a 5 mm \times 15 mm magnetic stir bar. The syringe pump was positioned so that the needle tip was approximately 2.5 cm above the CS solution. When the BX-CS dispersion was formed, 18 mL was obtained, and 2 mL of 0.1% TPP solution loaded in a syringe pump was then added dropwise (1 mL/min). The resulting suspension was continuously stirred at 1800 rpm for 30 min. An equal volume of acetate buffer (pH 5) was then added to make 40 mL of BX-CS/TPP suspension.

Formulation of BX-CS/TPP-HA MP

Ten (10) mL of the BX-CS/TPP suspension was gradually added dropwise into 10 mL of HA solution using a syringe pump (1 mL/min) fitted with a G21, 1-inch needle. A schematic of the preparation process is shown in Figure 1. The mixture was stirred continuously at room temperature for 30 min at 1800 rpm with a 5 mm \times 15 mm magnetic stir bar. Formation of BX-CS/TPP-HA MPs was expected during this step. The resulting suspension was then equilibrated for 24 h before testing.

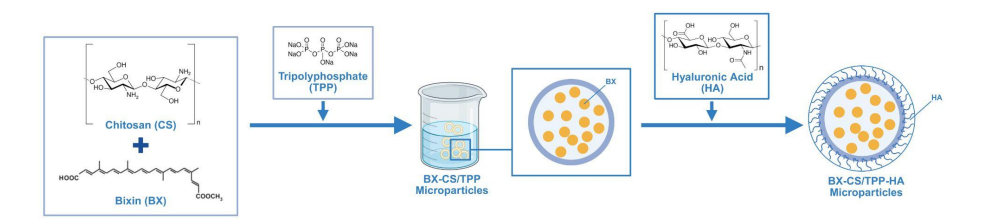


Figure 1: Flowchart for the preparation of BX-CS/TPP MPs

Preliminary Experiments

Preliminary experiments were conducted to determine the range of values for the factors that were used for the one-factor-at-a-time (OFAT) experiments. Different BX concentrations, CS:TPP ratios, and HA concentrations were investigated to evaluate their impact on the physical stability of the MPs and their tendency to form agglomerates. The range of each factor was determined through

visual inspection, ensuring the absence of visible agglomerates. The tested values for BX concentration, CS:TPP ratio, and HA concentration are presented in Table 1.

Table 1: Range of values for formulation factors evaluated in the preliminary experiments.

BX (mg/mL)	CS (g)	TPP (g)	CS:TPP Ratio (w:w)	HA % (w/v)
6.0	0.207	0.1	2:1	0.025
7.5	0.2588	0.1	2.5:1	0.05
9.0	0.3105	0.1	3:1	0.075
10.5	0.3623	0.1	3.5:1	0.1
12.0	0.414	0.1	4:1	0.5
13.5	0.4658	0.1	4.5:1	1.0
	0.5175	0.1	5:1	1.5
	0.621	0.1	6:1	

OFAT Experiments

The ranges determined from the preliminary experiments were used in the OFAT experiments to assess how varying a single factor influences a response and to observe whether these variations produced parabolic effects, such as peaks and troughs. The experiments were conducted by varying the value of one factor while keeping the others constant at their respective midpoints. The factors investigated include BX concentration (mg/mL), CS:TPP ratio (w:w), and HA concentration (% w/v). The specifications used are summarized in Table 2.

Particle size, PDI, and zeta potential in the OFAT experiments were measured using a dynamic light scattering analyzer (Zetasizer Ultra, Malvern Panalytical Ltd., Worcestershire, UK). This distinction is noted because, in a separate section of the study, measurements during the confirmatory steps were carried out using the Zetasizer Pro, which was available in the laboratory.

Table 2: Range of values for formulation factors evaluated in the OFAT experiments.

Factor			Levels		
BX (mg/mL)	6	7.5	9	10.5	12
CS:TPP Ratio (w:w)	3.5:1	3.75:1	4:1	4.25:1	4.5:1
HA (%w/v)	0.1	0.3	0.5	0.7	0.9

The effects of BX concentration, CS:TPP ratio, and HA concentration were evaluated based on the absence of agglomerates, particle size, polydispersity index (PDI), and zeta potential. In selecting the values to be used in the succeeding experiments, priority was given first to the absence of visible agglomerates, followed by the particle size, PDI, and zeta potential. Table 3 summarizes the prioritization of these factors and their acceptance criteria.

Table 3: Order of priority and acceptance criteria for each formulation factor

Factor	Order of Importance	Acceptance Criteria
Absence of agglomerates	1	No visible agglomerates
Particle Size	2	100 nm to 1000 μm (Khanthaphixay, Wu, & Yoon, 2023)
PDI	3	Not greater than 0.7 (Danaei et al., 2018)
Zeta Potential	4	-20 mV to -40 mV for moderately stable particles (Sizochenko et al., 2021)

Confirmatory Experiments

Formulation combinations were then developed based on the values identified from the OFAT experiments. These combinations were first evaluated for physical stability by checking for visible agglomerates. The formulation that showed no agglomeration was selected for further characterization, including particle size, PDI, zeta potential, as well as its encapsulation efficiency (EE) and loading capacity (LC). The formulation was also analyzed using Fourier transform infrared (FTIR) spectroscopy and scanning electron microscopy (SEM).

Characterization of BX-CS/TPP-HA MP

Particle Size, PDI, and Zeta Potential

The particle size, PDI, and zeta potential of the HA-coated BX-CS/TPP-HA MP formulation were determined using a dynamic light scattering analyzer (Zetasizer Pro, Malvern Panalytical Ltd., Worcestershire, UK). The instrument has a built-in software (ZS EXPLORER v.4.0.0.683) that performs the data processing and statistical analysis. Freshly prepared samples of BX-CS/TPP-HA MP suspension were first diluted with water (1:1) before analysis.

Functional Group Analysis using FTIR

To assess potential chemical interactions and confirm BX loading, FTIR spectra were obtained for BX-loaded MPs, pure BX, CS, HA, TPP, and BX-free MPs using an IR spectrophotometer using an attenuated total reflectance technique (IRSpirit with QATR accessory, Shimadzu, Kyoto, Japan). The spectra were recorded in the range of 4000–400 cm⁻¹.

<u>EE and LC</u>

The microparticle suspension was ultracentrifuged at 29,000 rpm (ThermoScientific Sorvall WX100, Thermo Fisher Scientific Inc., Langenselbold, Germany) for 1 h at 4°C to separate the supernatant from the MPs. The supernatant was collected with a micropipette and transferred to a 96-well plate for analysis. A blank solution, containing all components except BX, was prepared as a control. The absorbance was measured at 487 nm using a microplate reader (CLARIOstar MARS ver. 3.40R2, BMG Labtech GmbH, Germany).

The following formulas were used to calculate the EE and LC:

$$EE (\%) = \frac{Amount \ of \ BX \ initially \ added \ - \ Amount \ of \ BX \ in \ the \ supernatant}{Amount \ of \ BX \ initially \ added} \ x \ 100\%$$

$$LC (\%) = \frac{Amount \ of \ BX \ initially \ added \ - \ Amount \ of \ BX \ in \ the \ supernatant}{Mass \ of \ MPs} \ x \ 100\%$$

Morphological Analysis using SEM

The morphology was examined using an SEM (Model SU1500 SEM; Hitachi, Tokyo, Japan). To prepare the samples, distilled water was added to obtain 1 mL of 10%, 20%, and 50% dilutions. The samples were vortex-mixed for 30 s and sonicated for 3 min. Subsequently, 20 μL of each sample was placed on carbon tape mounted on a stub and allowed to dry overnight. The dried samples were coated with platinum using a Quorum Ion Sputter machine (U.K.) at 18 mA for 30 s. BX-CS/TPP-HA MPs were imaged at an accelerating voltage of 10 kV, magnifications ranging from 35× and 300× and a working distance of 11.4 - 11.6 mm.

Statistical Analysis

All experiments were carried out in triplicate. Data were presented as mean \pm standard deviation. SAS^{\circledast} OnDemand for Academics was the program used for statistical analyses. Welch ANOVA followed by Games-Howell post hoc tests were applied to compare the results, with p < 0.05 considered statistically significant.

RESULTS AND DISCUSSION

Preliminary Experiments

Acceptable Range of BX Concentrations

The maximum solubility demonstrated by BX in absolute ethanol, based on preliminary experiments, was 12 mg/mL. This was the highest concentration of BX used for the subsequent OFAT experiments.

Acceptable Range of CS:TPP ratios

CS:TPP ratios of 2:1, 2.5:1, and 3:1 produced clear dispersion, suggesting smaller particle sizes; however, agglomerates were formed. Larger agglomerates were also observed for ratios 5:1 and 6:1, suggesting physical instability. CS:TPP ratios 3.5:1, 4:1, and 4.5:1 resulted in turbid dispersion with no agglomerate formation, which was considered ideal. Therefore, for the subsequent OFAT experiments, CS:TPP ratios were set at 3.5:1, 3.75:1, 4:1, 4.25:1 and 4.5:1.

Acceptable Range of HA concentrations

HA concentrations of 0.025%, 0.05%, and 0.075% produced visible agglomerates when mixed with the BX-CS/TPP suspension. Concentrations above 2% were not tested due to excessive viscosity of the HA solutions. At 0.1%, 0.5%, and 1.0%, slightly turbid suspensions were obtained. However, agglomerates were observed in the 1.0% HA after 24 h equilibration. Based on these observations, the HA concentrations selected for the subsequent OFAT experiments were 0.1%, 0.3%, 0.5%, 0.7%, and 0.9% HA.

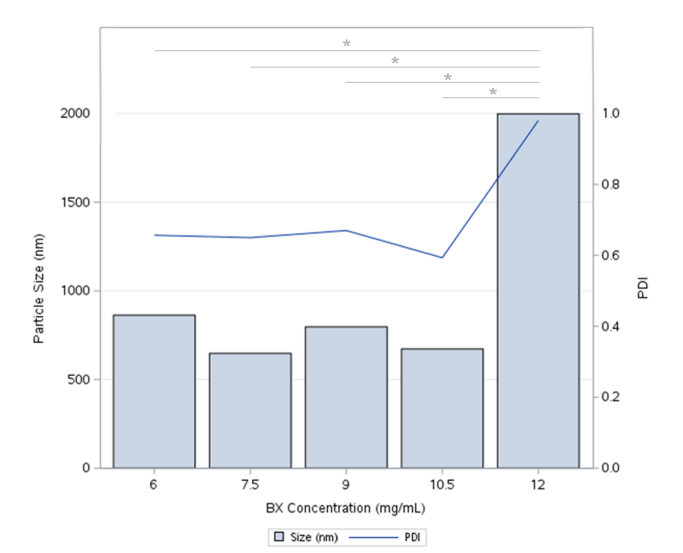
OFAT Experiments

Because of the limited number of microparticle-specific studies addressing the parameters investigated, several references cited in this discussion pertain to nanoparticles. However, fundamental principles of particulate drug delivery, such as diffusion-controlled release, matrix degradation, and polymer-drug interactions, are largely shared across both micro- and nanoscale systems.

Effect of BX concentration on BX-CS/TPP-HA MPs characteristics None of the prepared formulations exhibited visible agglomeration. However, MPs prepared using 12 mg/mL of BX resulted in significantly larger particles (Figure 2a).

MPs formulated from the 7.5 mg/mL BX achieved a desirable particle size but exhibited relatively low zeta potential (Figure 2a, 2b), while those prepared with 6 mg/mL BX had larger particle sizes compared with other trials. Consequently, BX concentrations of 6 mg/mL, 7.5 mg/mL, and 12 mg/mL were not considered for

further formulations. As shown in Figure 2, MPs prepared with 9 mg/mL and 10.5 mg/mL BX met all acceptance criteria for agglomeration, particle size, PDI, and zeta potential and were identified as the most suitable concentrations.



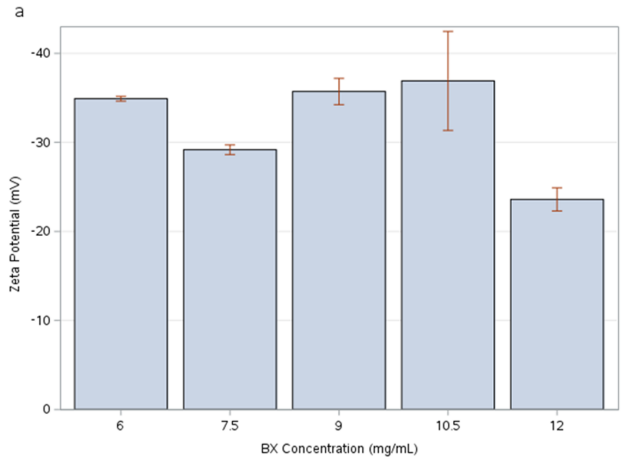


Figure 2: Effect of increasing bixin concentration on particle size together with PDI (a) and zeta potential (b) of BX-CS/TPP-HA MP. Data are presented as the mean (\pm SD) from three replicates. * p < 0.05 indicates a significant difference in particle size compared with other formulations.

Effect of CS:TPP ratio on BX-CS/TPP-HA MPs characteristics

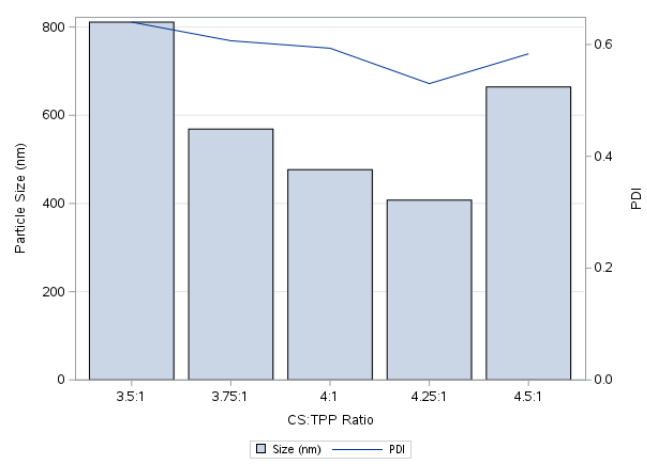
To evaluate the effect of the CS:TPP ratio on BX-CS/TPP-HA MP characteristics, five formulations with varying CS:TPP ratios from 3.5:1 to 4.5:1 were prepared using fixed BX and HA concentrations of 9 mg/mL and 0.50%, respectively. Among the formulations, CS:TPP ratios of 3.75:1 and 4.5:1 showed visible agglomeration. All CS:TPP ratios produced particles with sizes that were less than 1000 μm (based on Table 3), with the ratio 3.5:1 producing the largest particle size of 811.07 \pm 292.46 nm.

It was observed that decreasing the CS:TPP ratio below a certain threshold increased particle size, leading to particle agglomeration (Sreekumar, Goycoolea, Moerschbacher & Rivera-Rodriguez, 2018). A possible explanation is that lower CS:TPP ratios promote faster crosslinking, which may result in less-controlled particle formation (Chiesa et al., 2019). Such uncontrolled formation can lead to a greater proportion of large, undesirably sized nanoparticles.

As shown in Figure 3a, all CS:TPP ratio levels produced PDI values within the mid-range of 0.5-0.7. Higher CS:TPP ratios correspond to lower PDI, which may be attributed to reduced

crosslinking density, leading to slower and more controlled particle formation (Chiesa et al., 2019).

In Figure 3b, all ratios yielded zeta potential values between -20 to -40 mV. The negative charge is likely due to HA coating on the MPs. A highly negative zeta potential enhances stability in aqueous media and supports long-term storage, indicating efficient HA adsorption (Kalam, 2016). Overall, the CS:TPP ratio had a marked effect on particle size and PDI. Increasing the CS:TPP ratio led to gradual decreases on both parameters up to 4.5:1. However, ratio levels 4:1 and 4.25:1 showed lower zeta potentials, possibly due to agglomeration during HA adsorption, possibly linked to insufficient electrostatic stabilization which has also been observed in studies by Chiesa et al. (2018) and Nokhodi et al. (2022).



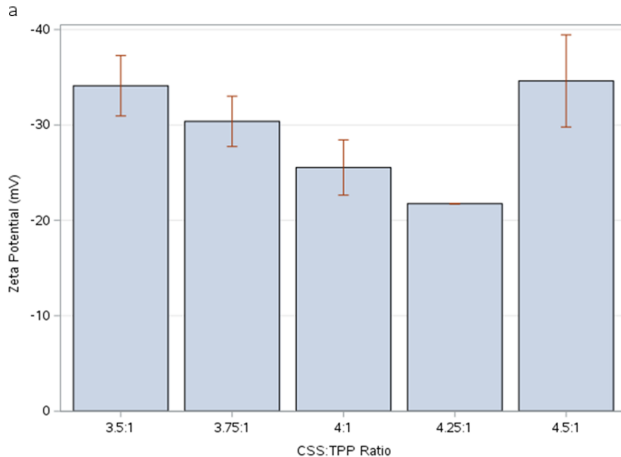
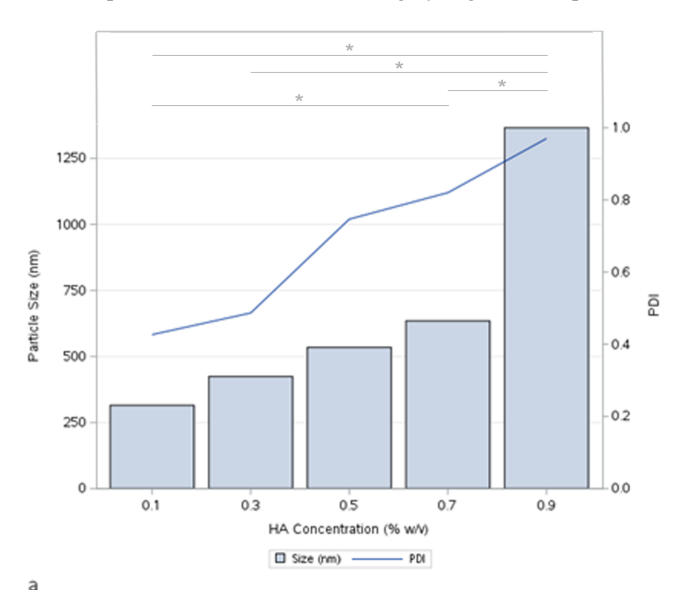


Figure 3: Effect of increasing CS:TPP ratio on particle size with PDI (a) and zeta potential (b) of BX-CS/TPP-HA MP. Data are presented as the mean (\pm SD) from three replicates. *p < 0.05 indicates a significant difference in particle size compared with other formulations.

Based on the results shown in Figure 3, CS:TPP ratios 4:1 and 4.25:1 were selected as they yielded the smallest particle sizes without visible agglomeration. Although the 3.5:1 also showed no agglomeration, it produced the largest particle size. In contrast, the 3.75:1 and 4.5:1 ratios exhibited physical instability with agglomeration and larger particle sizes.

Effect of HA Concentration on BX-CS/TPP-HA MPs characteristics. To evaluate the effect of HA concentration on BX-CS/TPP-HA MP characteristics, five formulations were prepared with HA concentrations ranging from 0.1 to 0.9 % w/v using fixed BX concentration (9 mg/mL) and CS:TPP ratio of (4:1). As shown in Figure 4a, particle size and PDI gradually increased with HA concentration with a steep increase at 0.9%. Particle size and PDI at 0.1%, 0.3%, and 0.7% HA differed significantly from those at 0.9%.

Considering zeta potential, HA concentrations of 0.3% and 0.7% yielded more negative values, suggesting better stability than 0.1%, 0.5%, and 0.9%. These values fall within the suggested range reported by Sizochenko et al. (2021). None of the formulations exhibited visible agglomeration. Based on these results, 0.3% HA was identified as the most suitable concentration, producing the smallest particle size, low PDI, and a highly negative zeta potential.



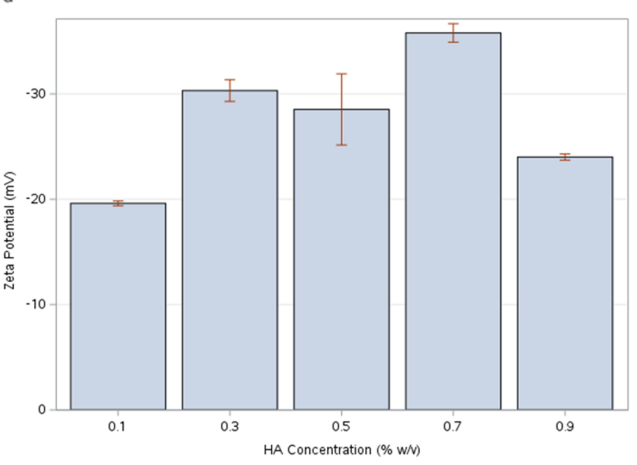


Figure 4: Effect of increasing HA concentration on particle size with PDI (a) and zeta potential (b) of BX-CS/TPP-HA MP. Data are presented as the mean (\pm SD) from three replicates. *p < 0.05 indicates a significant difference in particle size compared with other formulations.

Confirmatory Experiments

From the OFAT experiments, the following values were identified as suitable, and different combinations were tested for physical stability based on the absence of agglomerates. As shown in Table 4, trial formulation 1 9 mg/mL of BX, a CS:TPP ratio of 4:1, and 0.3% HA), was the most stable, showing no agglomeration. In contrast, precipitation was observed in other formulations, likely due to incompatibility between CS and HA contents. Agglomeration can occur through electrostatic interactions between positively charged CS MPs and negatively charged HA (Kalam, 2016c). At certain CS:HA ratios, stronger charge interactions may reduce zeta potential, leading to agglomeration and subsequent precipitation.

Table 4: Formulation combinations based on the OFAT experiments.

		_		
Formulation	BX (mg/mL)	CS:TPP ratio (w:w)	HA (%w/v)	Agglomeration
1	9	4:1	0.3	Absent
2	9	4:1	0.5	Present
3	9	4.25:1	0.3	Present
4	9	4.25:1	0.5	Present
5	10.5	4:1	0.3	Present
6	10.5	4:1	0.5	Present
7	10.5	4.25:1	0.3	Present
8	10.5	4.25:1	0.5	Present

FTIR Spectroscopy Analysis

The FTIR spectra in Figure 5 for BX and the microencapsulation materials used (CS, HA, and TPP) were consistent with their respective structures. When compared with the spectrum of BXfree MPs (CS/TPP-HA MPs), characteristic peaks of CS and HA remained observable. However, it can be noted that peaks of TPP attributed to its P=O and P-O stretching at 1130, 1211, and 880 cm-1 disappeared or had reduced intensity. This result is caused by the cross-linking reaction between the phosphate groups of TPP and the amine groups of CS. This confirms the successful ionic cross-linking during the preparation of the MPs by the mechanism of ionic gelation. This is further supported by the notable broadening of the N−H and O−H peaks centered at 3308 cm−1. This broadening is likely due to the electrostatic interaction between the amine groups, which are now in their charged form (-NH₃⁺), with the phosphate groups of TPP, confirming the ionic nature of the interaction.

The spectra of the BX-loaded MPs (BX-CS/TPP-HA MPs), on the other hand, can be seen to be very similar to the HA-CS/TPP MPs, retaining all characteristic peaks of CS, HA, and the disappearance and reduced intensity of the phosphate peaks from TPP, as well as the broadening of the N-H and O-H peaks. This suggests that, even with BX present, the MPs are still formed through ionic interactions between the amine groups of CS and phosphate groups of TPP. A notable difference with the BX-free MP spectrum is the appearance of peaks similar to the BX spectrum. Most notable is the appearance of the BX peak at 1653 cm—1. This result confirms that BX was successfully loaded and is present in the BX-CS/TPP-HA MPs prepared by ionic gelation.

Table 5: Summary of FTIR Responses

Group frequency wavenumber		Functional Group Assignment	Frequency wavenumber (cm-1)					
(cm-1) (Skoog, Holler & Crouch, 2007; Ferreira Tomaz et al., 2018)			BX	CS	НА	TPP	CS/TPP-HA MPs	BX-CS/TPP-HA MPs
800	P-O stretch	phosphoryl	-	-	-	880	880 (reduced intensity)	-
1000-1150	P=O stretch	phosphoryl	-	-	-	1130 1211	1130 1211 (reduced intensity)	-
1163-1210	C-O stretching	ester	1033	-	-	-	-	-
1180-1360	glucosamine	sugar moiety	-	1067	-	-	1070	-
1180-1360	N-acetylglucosamine	sugar moiety	-	1026	-	-	1035	-
1180-1400	C-N stretching	amine	-	1373	-	-	-	-
1650-1680	C=O stretching	amide	-	-	1603	-	1616	-
1720-1740	C=O stretching	carboxylic acid	1653	-	-	-	-	1653
2980-3095	C-H stretching	alkene	2988	-	-	-	2932	2926
2200 2700	O-H stretching	carboxylic acid	3447	-	3229	-	3308 (broadening)	-
3200-3600	O-H stretching	alcohol	-	3302	-	-	3308 (broadening)	-
3300-3500	N-H stretching	amine	-	3302	-	-	3308 (broadening)	-

342 SciEnggJ Vol. 18 | No. 02 | 2025

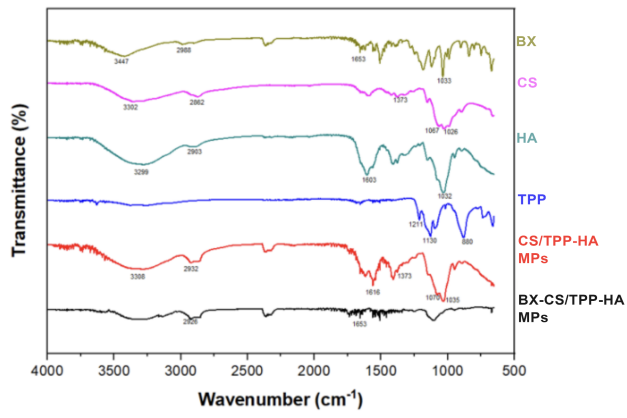


Figure 5: FTIR spectra of BX, CS, TPP, HA, BX-free MPs, and the BX-loaded MPs

Particle Size, PDI, and Zeta Potential of the Selected Formulation The study used dynamic light scattering (DLS) to measure particle size, PDI, and zeta potential, which provides quick and relatively low-cost measurements of particles. This is the main reason why it is the preferred method for particle size measurement (Bootz et al., 2004). As shown in Table 6, particles from Trials 1 and 3 met all acceptance criteria for the absence of visible agglomerates, particle size, PDI, and zeta potential. In contrast, Trial 2 exhibited visible agglomeration. This was reflected in the larger mean particle size, with the high standard deviation indicating the presence of particles of more than 1000 nm. The PDI standard deviation also exceeded the acceptance criterion of < 0.7, suggesting a very broad size distribution and marked variability among particle sizes in the suspension. It is important to note that while DLS is widely used for particulate characterization, it was not an appropriate tool for accurately determining the size of BX-CS/TPP-HA in this study. DLS reports the hydrodynamic diameter of particles in suspension and is better suited for nanoscale systems. A key limitation is that the size indicated in the software doesn't specifically reflect the true particle dimensions and morphology (Malvern Panalytical, 2019). For this reason, SEM was used to validate and confirm particle size, size distribution, shape, and surface texture.

Table 6: Physicochemical characteristics of the representative formulation consisting of (9 mg/mL BX, 4:1 CS:TPP ratio, 0.3% HA)

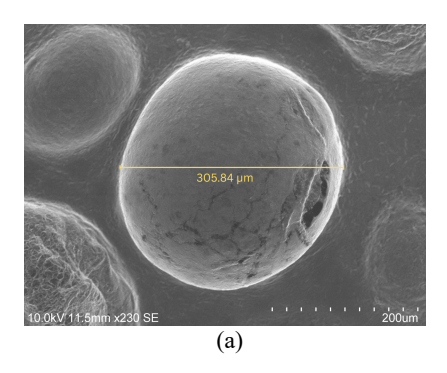
Trial	Agglomeration	Particle Size (nm)	PDI	Zeta Potential (mV)	Encapsulation Efficiency (%)	Loading Capacity (%)
1	Absent	539 ± 14.36	0.63 ± 0.02	-24.20 ± 2.21	65.27 ± 14.38	10.27 ± 2.26
2	Present	699.53 ± 419.30	0.65 ± 0.19	-22.16 ± 0.46	53.24 ± 15.17	9.66 ± 2.75
3	Absent	498.33 ± 5.18	0.65 ± 0.02	-26.82 ± 0.76	51.82 ± 8.13	12.54 ± 1.97

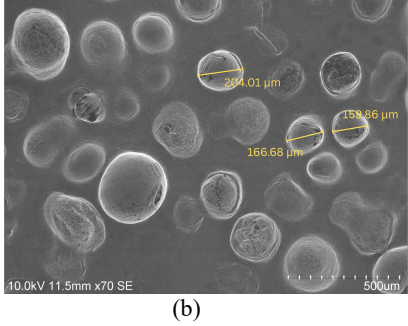
Note. Data are presented as the mean (\pm SD). Values are presented as mean \pm

Morphological Analysis using SEM

SEM provides a direct visualization of particle morphology under dry conditions, allowing for a more accurate measurement of actual particle dimensions (Bootz et al., 2004). Figure 6 shows SEM images taken at various magnifications. Particle size measurements using ImageJ (Version 1.54 g) ranged from 150 to 400 μ m,

confirming that the particles produced are indeed microparticles. The MPs exhibited slight elongation and rough surfaces, which may have resulted from dehydration before SEM analysis. This aligns with a known disadvantage of the technique, as drying can alter particle properties (Bootz et al., 2004).





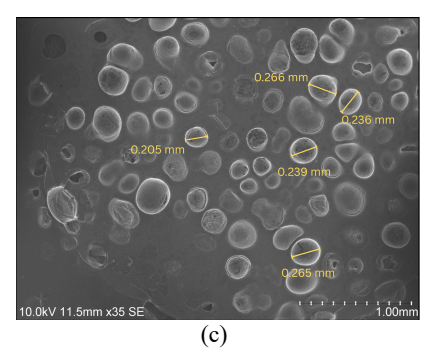


Figure 6: SEM images of the BX-CS/TPP-HA MPs at (a) 230x, (b) 70x, and (c) 35x magnification

Figure 7 shows the particle size distribution of 55 BX-CS/TPP-HA MPs, which were visible from the SEM sample pictures under 35× magnification. Majority of the particles (72.73%) are under the peak of the curve, measuring 0.20-0.25 mm. The data followed a normal distribution curve.

A combination of DLS and SEM is widely recommended for studying particles. DLS is useful for determining mean particle size, PDI, and zeta potential, while SEM provides detailed

morphological characterization, including particle shape and surface texture, and also confirms individual particle sizes. In addition, when coupled with image analysis software, SEM can be used to assess particle size distribution.

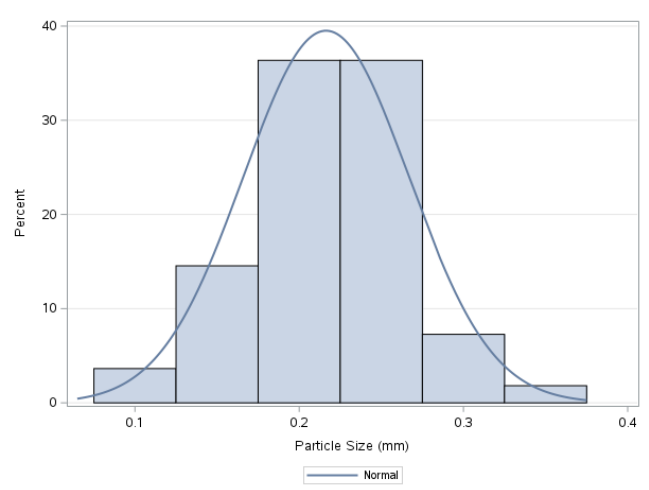


Figure 7: Particle size distribution of the BX-CS/TPP-HA MPs

EE and LC

EE and LC of the MPs were evaluated to determine the amount of the BX encapsulated. For trials 1, 2, and 3, the EE values were relatively high at $65.27 \pm 14.38\%$, $53.24 \pm 15.17\%$, and $51.82 \pm 14.38\%$ 8.13% (Table 6). Assessing EE is essential to determine the efficiency of the encapsulation procedure, as higher EE values imply that there is minimal loss of the active compound during the loading process (Trushina et al., 2022). The relatively high EE observed in the formulations may be attributed to the formation of an amorphous complex with the HA-coated matrix (Meylina et al., 2023).

For LC, Trials 1, 2, and 3 yielded values of $10.27 \pm 2.26 \%$, 9.66 \pm 2.75%, and 12.54 \pm 1.97%, respectively. LC reflects the proportion of BX relative to the total MP weight, indicating the amount of BX encapsulated per particle. The relatively low LC observed suggests that only small amounts of BX are entrapped, which may require higher quantities of MPs to achieve the desired pharmacological concentration. This information is particularly useful in estimating the potential BX content in various dosage forms.

CONCLUSION

In this study, BX-loaded HA-coated CS/TPP MPs were prepared using the ionic gelation method. Furthermore, we determined the potential effects of the formulation factors on the characteristics of the MPs. Particle size and PDI increase with increasing BX and HA

concentrations. MPs prepared using BX and HA concentrations greater than 9 mg/mL and 0.9% w/v may lead to particle agglomeration. On the other hand, increasing the CS:TPP ratio up to 4.25:1 leads to an increase in particle size and PDI. The zeta potential values of the MPs produced in the OFAT experiments were all within the acceptable range for moderate stability of the particles.

Preparing the MPs using selected formulation factors of 9 mg/mL BX, 4:1 CS:TPP ratio, 0.3% HA resulted in MPs of desirable particle size, PDI, and zeta potential. The effects of other factors, such as preparation parameters like sonication or mixing speed, can also be further explored to achieve more consistent results and determine their impact on the desired endpoints.

The results of this study can be used as a basis for further evaluation of the factors and optimization of the BX-loaded HA-coated CS/TPP MP using techniques such as screening/characterization and response surface methodology, respectively.

ACKNOWLEDGMENT

This study was funded by the UP System Enhanced Creative Work and Research Grant (ECWRG 2020-2-1R) under the Office of the Vice President for Academic Affairs, University of the Philippines, awarded to Bienvenido Balotro in 2021.

The authors sincerely thank the following individuals for their support and assistance in the completion of this research: Brandon Belmi and the students of the Pharm Sci 187 laboratory class during the Second Semester, Academic Year 2022-2023, for their participation in the preliminary exercises related to the formulation of bixin microparticles; Kristian Jude Borres and Mark Mangogtong of DKSH Philippines for sharing their company resources; Bernard Jude Gutierrez and Madelaine L. Ebarvia of the Department of Science and Technology-Industrial Technology Development Institute, Environmental and BioEngineering Unit for assisting in the use of the refrigerated ultracentrifuge in their laboratory.

CONFLICT OF INTEREST

All authors declare no conflicts of interest.

Authors	Provided the original idea	Wrote the draft of the manuscript and significant revisions	Participated in data gathering	Performed stat analysis	Substantial contribution
Bienvenido Balotro	X	X	X		X
Sean Paul Rojo		X	X	X	X
Keane Mc Josef Ku		X	X	X	X
Jude Benedick Acedera		X	X	X	X
Ma. Cailah Velasco		X	X	X	X
Cherika Eunyce Catalogo		X	X	X	X
Danielle Justinne Clemente		X	X	X	X
Shanna Nicole Ong		X	X	X	X
Bryan Paul Bulatao	X	X	X		X
Patrick Junard Regidor			X	X	X
Clinton Gomez	X	X	X		X

Authors	Provided the original idea	Wrote the draft of the manuscript and significant revisions	Participated in data gathering	Performed stat analysis	Substantial contribution
Czarina Dominique Delos	X	X	X		X
Santos					
Ethel Andrea Ladignon	X	X			X
Jocelyn Palacpac	X	X			X
Julius Andrew Nunez			X	X	X

REFERENCES

- Almalik, A., Donno, R., Cadman, C. J., Cellesi, F., Day, P. J., & Tirelli, N. (2013). Hyaluronic acid-coated chitosan nanoparticles: Molecular weight-dependent effects on morphology and hyaluronic acid presentation. *Journal of Controlled Release*, 172(3), 1142–1150. https://doi.org/10.1016/j.jconrel.2013.09.032
- Bonferoni, M. C., Sandri, G., Gavini, E., Rossi, S., Ferrari, F., & Caramella, C. (2007). Microparticle systems based on polymer-drug interaction for ocular delivery of ciprofloxacin I. *In vitro* characterization. *Journal of Drug Delivery Science and Technology*, 17(1), 57–62. https://doi.org/10.1016/S1773-2247(07)50008-0
- Bootz, A., Vogel, V., Schubert, D., & Kreuter, J. (2004). Comparison of scanning electron microscopy, dynamic light scattering and analytical ultracentrifugation for the sizing of poly(butyl cyanoacrylate) nanoparticles. *European Journal of Pharmaceutics and Biopharmaceutics*, 57(2), 369–375. doi:10.1016/s0939-6411(03)00193-0
- Camelo, S., Latil, M., Veillet, S., Dilda, P. J., & Lafont, R. (2020). Beyond AREDS formulations, what is next for intermediate agerelated macular degeneration (iAMD) treatment? potential benefits of antioxidant and anti-inflammatory apocarotenoids as neuroprotectors. *Oxidative Medicine and Cellular Longevity*, 2020, 4984927. https://doi.org/10.1155/2020/4984927
- Chiesa, E., Dorati, R., Conti, B., Modena, T., Cova, E., Meloni, F., & Genta, I. (2018). Hyaluronic Acid-Decorated Chitosan Nanoparticles for CD44-Targeted Delivery of Everolimus. *International Journal of Molecular Sciences*, 19(8), 2310. https://doi.org/10.3390/ijms19082310
- Des Bouillons-Gamboa, R. E., Montes de Oca, G., Baudrit, J. R. V., Ríos Duarte, L. C., Lopretti, M., Rentería Urquiza, M., Zúñiga-Umaña, J. M., Barreiro, F., & Vázquez, P. (2024). Synthesis of chitosan nanoparticles (CSNP): Effect of CH-CH-TPP ratio on size and stability of NPs. Frontiers in Chemistry, 12. https://doi.org/10.3389/fchem.2024.1469271
- de Oliveira Júnior, R. G., Bonnet, A., Braconnier, E., Groult, H., Prunier, G., Beaugeard, L., Grougnet, R., da Silva Almeida, J. R. G., Ferraz, C. A. A., & Picot, L. (2019). Bixin, an apocarotenoid isolated from Bixa orellana L., sensitizes human melanoma cells to dacarbazine-induced apoptosis through ROS-mediated cytotoxicity. Food and Chemical Toxicology: An International Journal Published for the British Industrial Biological Research Association, 125, 549–561. https://doi.org/10.1016/j.fct.2019.02.013
- Dragostin, I., Dragostin, O.-M., Iacob, A. T., Dragan, M., Chitescu, C. L., Confederat, L., Zamfir, A.-S., Tatia, R., Stan, C. D., & Zamfir, C. L. (2022). Chitosan Microparticles Loaded with New Non-Cytotoxic Isoniazid Derivatives for the Treatment of

- Tuberculosis: In Vitro and In Vivo Studies. *Polymers*, 14(12), Article 12. https://doi.org/10.3390/polym14122310
- EFSA Panel on Food Additives and Nutrient Sources added to Food (ANS). (2016). The safety of annatto extracts (E 160b) as a food additive. *EFSA Journal*, *14*(8), e04544. https://doi.org/10.2903/j.efsa.2016.4544
- Espinosa-Cano, E., Huerta-Madroñal, M., Cámara-Sánchez, P., Seras-Franzoso, J., Schwartz, S., Abasolo, I., San Román, J., & Aguilar, M. R. (2021). Hyaluronic acid (HA)-coated naproxennanoparticles selectively target breast cancer stem cells through COX-independent pathways. *Materials Science and Engineering:* C, 124, 112024. https://doi.org/10.1016/j.msec.2021.112024
- Ferreira Tomaz, A., Sobral de Carvalho, S. M., Cardoso Barbosa, R., L. Silva, S. M., Sabino Gutierrez, M. A., B. de Lima, A. G., & L. Fook, M. V. (2018). Ionically Crosslinked Chitosan Membranes Used as Drug Carriers for Cancer Therapy Application. *Materials*, 11(10), 2051. https://doi.org/10.3390/ma11102051
- Husa, N. N., Hamzah, F., & Said, H. M. (2018). Characterization and Storage Stability Study of Bixin Extracted from Bixa orellana Using Organic Solvent. IOP Conference Series: Materials Science and Engineering, 358(1), 012035. https://doi.org/10.1088/1757-899X/358/1/012035
- Kalam, M. A. (2016). Development of chitosan nanoparticles coated with hyaluronic acid for topical ocular delivery of dexamethasone. *International Journal of Biological Macromolecules*, 89, 127–136. https://doi.org/10.1016/j.ijbiomac.2016.04.070
- Khanthaphixay, B., Wu, L., & Yoon, J. Y. (2023). Microparticle-Based Detection of Viruses. *Biosensors*, 13(8), 820. https://doi.org/10.3390/bios13080820
- Kim, E. S., Baek, Y., Yoo, H.-J., Lee, J.-S., & Lee, H. G. (2022). Chitosan-tripolyphosphate nanoparticles prepared by ionic gelation improve the antioxidant activities of astaxanthin in the in vitro and in vivo model. *Antioxidants*, 11(3), 479. https://doi.org/10.3390/antiox11030479
- Malvern Panalytical (2019). Zetasizer ultra/pro user guide. Malvern Panalytical Ltd. Worcestershire, UK.
- Meylina, L., Muchtaridi, M., Joni, I. M., Elamin, K. M., & Wathoni, N. (2023). Hyaluronic acid-coated chitosan nanoparticles as an active targeted carrier of alpha mangostin for breast cancer cells. *Polymers*, 15(4), 1025. https://doi.org/10.3390/polym15041025
- Moreira, P. R., Maioli, M. A., Medeiros, H. C. D., Guelfi, M., Pereira, F. T. V., & Mingatto, F. E. (2014). Protective effect of bixin on carbon tetrachloride-induced hepatotoxicity in rats.

- Biological Research, 47(1), 49. https://doi.org/10.1186/0717-6287-47-49
- Parajó, Y., D'Angelo, I., Welle, A., Garcia-Fuentes, M., & Alonso, M. J. (2010). Hyaluronic acid/Chitosan nanoparticles as delivery vehicles for VEGF and PDGF-BB. *Drug Delivery*, *17*(8), 596–604. https://doi.org/10.3109/10717544.2010.509357
- Sizochenko, N., Mikolajczyk, A., Syzochenko, M., Puzyn, T., Leszczynski, J. (2021). Zeta potentials (ζ) of metal oxide nanoparticles: A meta-analysis of experimental data and a predictive neural networks modeling. *NanoImpact*, 22. https://doi.org/10.1016/j.impact.2021.100317
- Skoog, D.A., Holler, F.J., Crouch, S.R. (2007) Principles of instrumental analysis. Thomson/Brooks Cole. Belmont, CA. p.461
- Stefansson, E. (2022). Eye drops for retinal disease. *Acta Ophthalmologica*, 100(S275). https://doi.org/10.1111/j.1755-3768.2022.15618
- Tanito, M., Hara, K., Takai, Y., Matsuoka, Y., Nishimura, N., Jansook, P., Loftsson, T., Stefánsson, E., & Ohira, A. (2011). Topical Dexamethasone-Cyclodextrin Microparticle Eye Drops for Diabetic Macular Edema. *Investigative Ophthalmology & Visual Science*, 52(11), 7944–7948. https://doi.org/10.1167/iovs.11-8178
- Tao, S., Park, S. L., Rojo de la Vega, M., Zhang, D. D., & Wondrak, G. T. (2015). Systemic administration of the apocarotenoid bixin protects skin against solar UV-induced damage through activation of NRF2. Free Radical Biology & Medicine, 89, 690–700. https://doi.org/10.1016/j.freeradbiomed.2015.08.028
- Trushina, D. B., Borodina, T. N., Belyakov, S., & Antipina, M. N. (2022). Calcium carbonate vaterite particles for drug delivery: Advances and challenges. *Materials Today Advances*, 14, 100214. https://doi.org/10.1016/j.mtadv.2022.100214
- Tsuruma, K., Shimazaki, H., Nakashima, K.-I., Yamauchi, M., Sugitani, S., Shimazawa, M., Iinuma, M., & Hara, H. (2012). Annatto prevents retinal degeneration induced by endoplasmic reticulum stress in vitro and in vivo. *Molecular Nutrition & Food Research*, 56(5), 713–724. https://doi.org/10.1002/mnfr.201100607